Spectrum of quasistable states in a strong microwave field

A. Arakelyan,[1] T. Topcu,[2,3] F. Robicheaux,[2,*] and T. F. Gallagher[1]

[1]*Department of Physics, University of Virginia, Charlottesville, Virginia 22904, USA*

[2]*Department of Physics, Auburn University, Auburn, Alabama 36849, USA*

[3]*Department of Physics, University of Nevada, Reno, Nevada 89557, USA*

When atoms are exposed to intense laser or microwave pulses, $\sim$10% of the atoms are found in Rydberg states subsequent to the pulse, even if it is far more intense than required for static field ionization. The optical spectra of the surviving Li atoms in the presence of a 38-GHz microwave field suggest how atoms survive an intense pulse. The spectra exhibit a periodic train of peaks 38 GHz apart. One peak is just below the limit, and with a 90-V/cm field amplitude the train extends from 300 GHz above the limit to 3000 GHz below it. The spectra and quantum-mechanical calculations imply that the atoms survive in quasistable states in which the Rydberg electron is in a weakly bound orbit infrequently returning to the ionic core during the intense pulse.

I. INTRODUCTION

When ground-state atoms are ionized by an intense laser pulse, Rydberg atoms can be produced as a byproduct [1]. Even when multiple ionization of the atom occurs, it can be accompanied by the production of ionic Rydberg states converging to higher ionization limits [2]. While the notion of producing weakly bound Rydberg states with an intense laser pulse might seem surprising, it can be understood in the following way. The intense laser pulse ejects the electron from the ion core either in a single field cycle, through tunnel ionization, or over many cycles, via multiphoton ionization (MPI). In either case, the electron departs from the core with a range of energies into the long-range tail of the Coulomb potential, where the electron is nearly free, and there is no cycle average energy exchange with the laser field. Above the ionization limit the range of energies appears explicitly in the form of above threshold ionization (ATI) [3], but the energy range extends below the limit as well. An electron with an energy below the limit is reflected by the Coulomb potential and returns to the core in one Kepler period [1,4,5]. If the laser pulse is over before the return, the electron obviously remains bound. If the laser pulse is not over, rescattering of the electron from the core can lead to superponderomotive ATI, recombination and high harmonic generation, nonsequential double ionization, and nearly elastic scattering. Nearly elastic scattering can result in a very low-energy free electron, as observed recently [6–8], or in a bound electron [3,9–12]. A striking example of the last process is provided by recent experiments with He in which 10% of the surviving atoms are attributed to states of principal quantum number $n < 7$ with Kepler orbital periods less than the 30-fs duration of the 1-GV/cm laser pulse [12].

How atoms survive an intense field was first addressed in calculations of high-frequency stabilization [13,14]. More recent calculations to elucidate the source of superponderomotive electrons in ATI are, however, more relevant to this problem [15]. Superponderomotive electrons are those with energies in excess of the prediction of the classical model used to describe ATI [16–18]. They are formed at the intensities at which the ac Stark shift from the laser field brings states just below the limit into multiphoton resonance with the ground state. At these intensities quasistable states are produced in which the atom survives multiple recollisions with the core, with some loss of population on each recollision [15].

Microwave ionization of Rydberg atoms exhibits many similarities to MPI of ground-state atoms. In particular, recent microwave ionization experiments have shown that 10% of the atoms remain bound in high-lying states at fields orders of magnitude beyond those required for static field ionization [19,20]. Furthermore, electrons in the high-lying states remain bound even if they return to the ionic core during the microwave pulse [19,20], essentially the same result as observed in the laser experiments [15]. While quasistable high-lying states are formed in both the laser and microwave experiments, an attractive feature of the microwave case is that it is possible to probe them spectrally. Here we report the optical excitation spectra of Rydberg atoms in a strong microwave field. Our spectra and calculations demonstrate that the surviving atoms result from excitation to microwave dressed states just below the limit. Specifically the spectra consist of series of peaks separated by the microwave frequency. These observations imply that the atoms are in quasistable states in which the stability derives largely from the electron's spending most of its time far from the ionic core. Nonetheless, the atom survives the electron's revisiting the core. In the sections which follow we describe our experimental approach, present our experimental observations, and show the results of one-dimensional quantum calculations of the spectra.

II. EXPERIMENTAL APPROACH

This section provides only a brief outline of the experimental apparatus used in the current experiment since a detailed description can be found elsewhere [19]. A thermal beam of Li atoms in its ground state passes through the antinode at the center of a 38.34-GHz Fabry-Perot cavity where the atoms are excited to the vicinity of the ionization limit by three 20-ns dye laser pulses via the $2s \rightarrow 2p \rightarrow 3s \rightarrow np$ transitions at wavelengths of 670, 813, and 615 nm, respectively. All three

---

*Current address: Department of Physics, Purdue University, West Lafayette, Indiana 47907, USA.
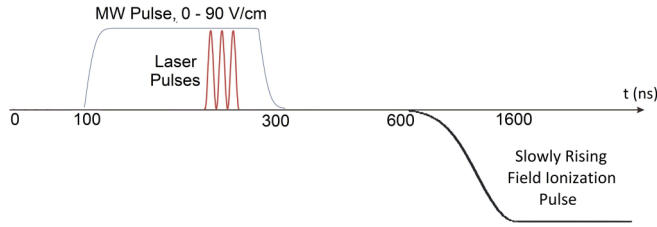
FIG. 1. (Color online) Experimental timing diagram for the investigation of the microwave recombination in Li by a 38.3-GHz microwave (MW) field.

laser pulses are 20 ns long. The second pulse overlaps the first, being delayed by only 5 ns from the first pulse. The third pulse begins 1–2 ns after the end of the second pulse. The experiment is run at a 500-Hz repetition rate. The laser excitation occurs in the presence of a microwave field, as shown in the timing diagram in Fig. 1, so the oscillator strength to the np states becomes nearly continuously distributed in energy. The microwave pulse starts before the laser excitation and lasts for a minimum of 20 ns after it. Unless stated otherwise, the microwave field is on for 30 ns after the pulsed laser excitation. The rise and fall times of the pulse are approximately 20 ns each. After the end of the microwave pulse, typically 300 ns later, atoms are field ionized by a field-ionization pulse, which reaches a maximum of 110 V/cm with a 1-μs rise time. It is adequate to fully ionize states of $n > 43$. The electrons ejected by the ionization field are detected by a dual microchannel plate detector (MCP). The time resolved MCP signal tells us how many atoms survived the microwave pulse in bound states, as well as their final state distribution. The MCP signal is captured by a gated integrator or oscilloscope and recorded for later analysis. The microwave system generates a 38.34-GHz pulse with a variable width and 0- to 90-V/cm amplitude, which is determined with an uncertainty of 15%. A stray field of 8 mV/cm is present in the excitation volume, and well-defined static fields can be added. A relative frequency measurement of the $3s \rightarrow np$ laser is obtained with the help of a 52.42-GHz free spectral range etalon, and an optogalvanic signal from the 16 274.0212-cm^{-1} $2p^5(2p_{3/2})3s$-$2p^5(2p_{3/2})2p$ Ne line provides an absolute calibration. The three laser beams are focused to less than 1-mm-diameter spots where they intersect the atomic beam. The 615-nm beam propagates perpendicularly to the 670- and 813-nm beams, so the volume of excited atoms is ≈ 1 mm^3. The laser fields and microwave field are polarized vertically.

III. OBSERVATIONS

In Fig. 2 we show the spectra obtained by scanning the frequency of the third laser in the presence of microwave fields from 0 to 45 V/cm. The gate of the integrator is wide enough to collect the field-ionization signals of all states of $n > 43$, that is, of energies greater than -1500 GHz. We specify energies relative to the zero-field ionization limit. In zero microwave field we observe resolved bound Rydberg states at energies lower than -300 GHz and a flat signal at higher energies, where the spacing between adjacent levels is smaller than
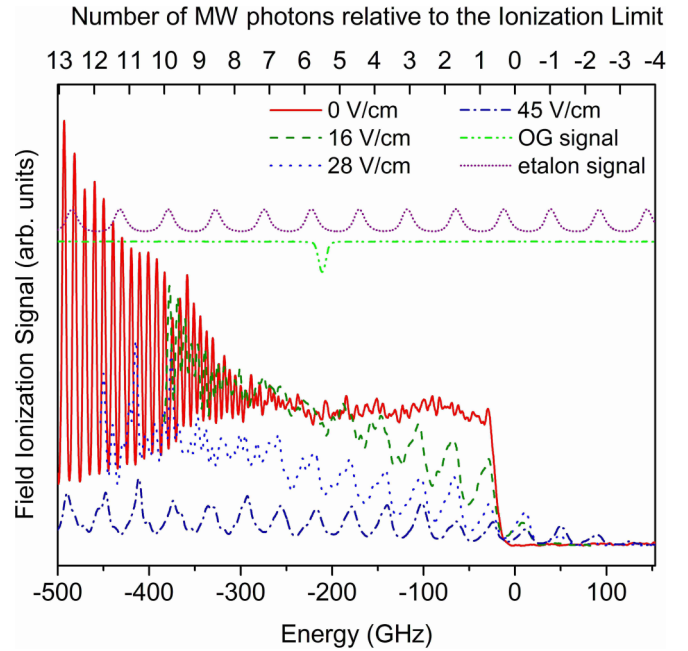

FIG. 2. (Color online) Field-ionization signal as a function of laser frequency tuning, in terms of energy relative to the ionization limit (IL), after exposure to a microwave pulse of amplitude 0, 16, 36, and 45 V/cm. The horizontal axis is calibrated by the etalon and optogalvanic signals.

the 8-GHz linewidth of our laser, which occurs at $n \approx 100$. At an energy of -45 GHz, the signal starts falling to zero because photoelectrons are not detected when the laser is tuned over the ionization limit. Due to the finite linewidth of the laser, the signal drops to zero with a finite slope, and we denote the middle of that slope as the ionization limit. The limit is depressed due to the stray static field in the interaction region mentioned above. We estimate the stray field using $\Delta W = 2\sqrt{E}$. We use atomic units unless other units are explicitly specified. Typically, the data are taken when the depressed ionization limit is at -18 GHz, which corresponds to a stray field of 8 mV/cm. As shown by Fig. 2, the presence of the microwave field leads to an obvious modulation of the spectrum at the microwave frequency. There are several points to note regarding Fig. 2. First, as the microwave field is raised the regular structure persists further both above and below the ionization limit, as observed previously [20–22]. Second, in the 16-V/cm spectrum of Fig. 2 the high-frequency side of the peak at the limit coincides with the drop in signal at the limit in the zero (microwave) field spectrum of Fig. 2. In addition, the peaks in the signal near the limit are asymmetric, but the asymmetry disappears at higher microwave fields. This asymmetry is expected if the ionization occurs through photon absorption in the perturbative limit (low power), since in this case the photoabsorption rate scales as $1/n^3$. This results in a higher photoionization rate for an electron bound by 95% of the photon energy than for one bound by 5% of the photon energy. Finally, the entire set of peaks moves to higher energy due to the ponderomotive energy shift. For the highest microwave field we have used, 90 V/cm, we observe a ponderomotive shift of 15 GHz, confirming our field calibration.
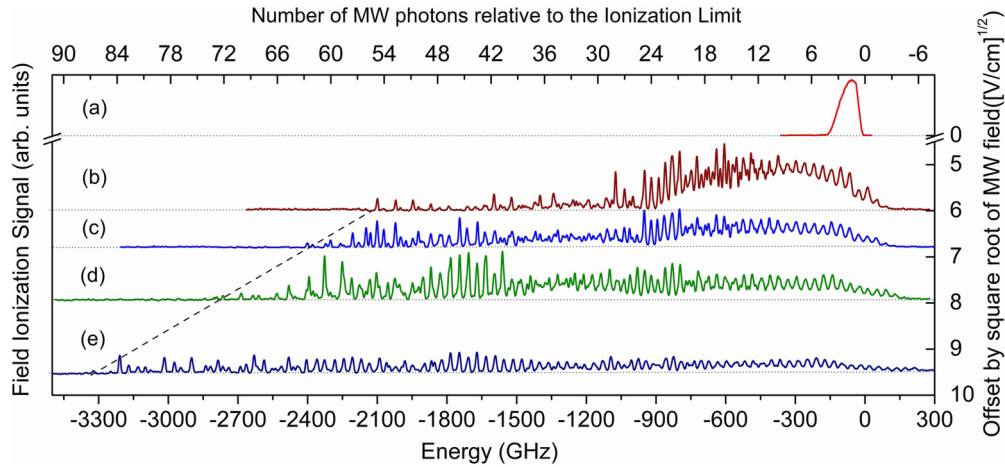
FIG. 3. (Color online) Field-ionization signal as a function of laser frequency, after exposure to a microwave pulse of amplitudes (a) 0 V/cm, (b) 36 V/cm, (c) 45 V/cm, (d) 63 V/cm, and (e) 90 V/cm. A 50-ns integration gate is used to detect only atoms bound within 75 GHz of the IL. The zero-field spectrum is scaled by a factor of 1/3 to fit the graph. Horizontal dotted lines show the zeros of the corresponding spectra. The traces are offset by the square root of the microwave field. The broken line connects the onsets of the peaks in the different spectra, and the energy of the onset obeys the relation $W = -4\sqrt{E}$.

Inspection of the time-resolved field-ionization signal obtained in the 45-V/cm trace of Fig. 2 shows that all the signal comes from atoms in very highly excited states. Accordingly we narrowed the gate of the integrator to 50 ns to detect only atoms bound by less than 75 GHz and recorded the spectra shown in Fig. 3. When there is no microwave field, we only detect a signal when the laser is tuned within 75 GHz of the depressed ionization limit at -18 GHz. It is important to bear in mind that 75 GHz is an upper limit to the binding energy of the atoms we detect. As the microwave field amplitude is increased the spectrum extends progressively further above the limit and, more interesting, to very deeply bound states. The

broken line of Fig. 3 connects the onsets of the peaks in the spectra, and the energy of the onset is linearly dependent on the square root of the microwave field. Converting from the laboratory units given in Fig. 3 to atomic units shows that the energy of the onset is given by $W = -4\sqrt{E}$, almost exactly twice the binding energy for classical field ionization. It is not clear to us why the onset of the spectra occurs at $W = -4\sqrt{E}$, but measurements at another frequency might clarify this point.

The regularity of the structure at the microwave frequency extends almost as far as the spectra shown in Fig. 3. In Fig. 4(b) we show an expanded view of the 90-V/cm spectrum of Fig. 3,
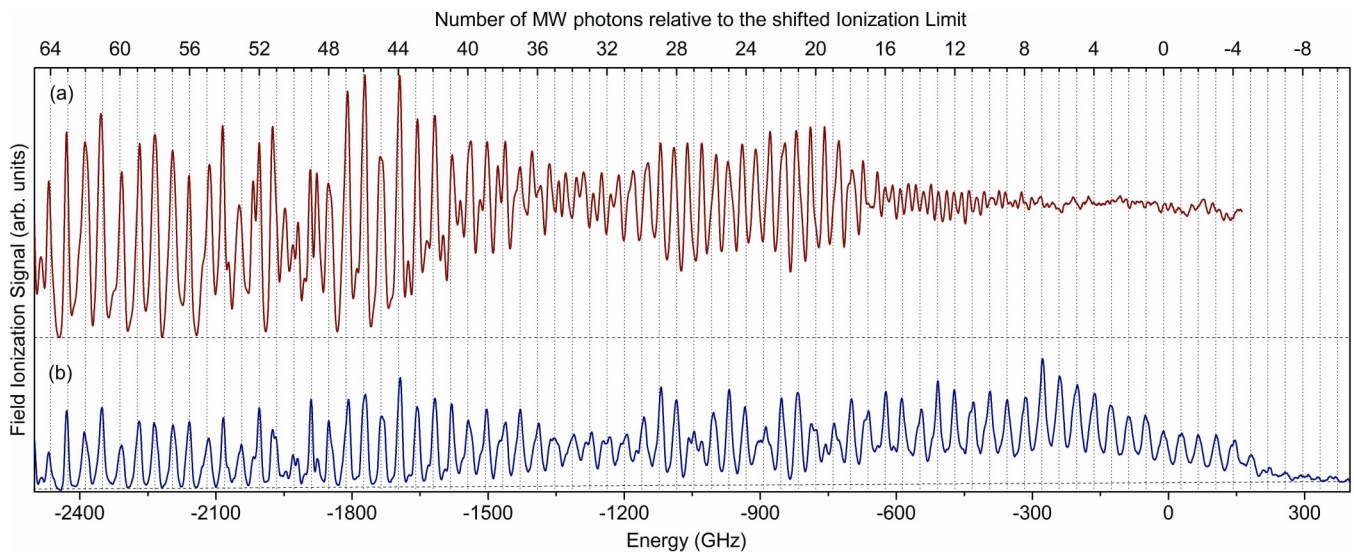

FIG. 4. (Color online) Field-ionization signals as a function of laser frequency for excitation in the presence of a microwave pulse of amplitude 90 V/cm. (a) The total photoabsorption spectrum when detecting all energies above $n = 43$. (b) Spectrum obtained when detecting only the high-lying states. The total photoabsorption spectrum is scaled by a factor of 8 to fit the graph. Horizontal dashed lines show the zeros of the corresponding spectra. The total photoabsorption spectrum also presents the 38-GHz structure at energies below -1500 GHz since only atoms transferred to higher-lying states are detected.

as well as a set of vertical dotted lines spaced by the microwave frequency to show the regularity of the microwave induced structure down to an energy of −2400 GHz. In Fig. 4(a) we show the spectrum recorded in the presence of a 90-V/cm microwave field when the atoms are ionized immediately, ∼10 ns, after the microwave pulse by a field pulse which ionizes atoms bound by up to 1500 GHz. Electrons produced by microwave ionization do not leave the interaction region in this time, so the resulting spectrum is identical to one obtained by detecting ions. At energies below −1500 GHz not all the initially excited atoms are detected, only ones which have been transferred to within 1500 GHz of the ionization limit. Thus the spectrum has the same modulation as the spectrum of Fig. 4(b), in which the field pulse is 300 ns after the microwave pulse, as shown in Fig. 1. At energies above −1500 GHz there is, in general, no obvious connection between the spectra of Figs. 4(a) and 4(b). An exception is the region near −900 GHz where there is a modulation in the spectrum of Fig. 4(a) at a slightly lower frequency than the microwave frequency. The microwave frequency matches the Kepler, $\Delta n = 1$, frequency at −1050 GHz, which is probably the origin of the structure in Fig. 4(a). In any event, the deep modulation of the total number of atoms excited, shown in Fig. 4(a), introduces a beat note into the spectrum of Fig. 4(b). Finally, the spectrum of Fig. 4(b) extends from the regime in which the microwave frequency is much larger than the $\Delta n = 1$ frequency, at the limit, to the regime in which it is smaller than the $\Delta n = 1$ frequency. For example, the Li $37p$ and $38p$ states, bound by 2409 and 2284 GHz, respectively, are separated by three times the microwave frequency.

Several observations suggest that the spectra are tied to the ionization limit. First, the spectra of Fig. 3 were recorded by detecting very high-lying states. Second, in Figs. 2 and 3 the extent of the spectra above and below the limit increases with the microwave field amplitude. Finally, the 16-V/cm spectrum of Fig. 2 appears to have a peak at the ionization limit. As an explicit test of this notion we have recorded spectra in the presence of small static fields which depress the limit by different amounts. In Fig. 5 we show segments of spectra recorded in static fields of up to 55 mV/cm. In particular, we show segments of the spectra at the limit and at the energy −1400 GHz. At the limit the spectra shift to lower energy as the depressed limit shifts, and precisely the same shift is observed at −1400 GHz. In short, the entire spectrum is tied to the ionization limit. The other important aspect of Fig. 5 is that the size of the peaks decreases with increasing static field, and the peaks essentially disappear at 55 mV/cm. The dependence on the static field suggests that atoms which survive the microwave field are in states within one microwave photon of the limit. A static field of 50 mV/cm depresses the ionization limit by 41 GHz, almost exactly the microwave frequency. We chose the energy −1400 GHz for Fig. 5 because it was the lowest energy at which structure persisted up to a static field of 40 mV/cm. Unfortunately, at this binding energy the Kepler frequency is close to the microwave frequency, and the observed structure is not simply composed of peaks displaced from the limit by multiples of the microwave frequency; there are small subsidiary peaks. The same phenomenon can be seen in Fig. 4(b).
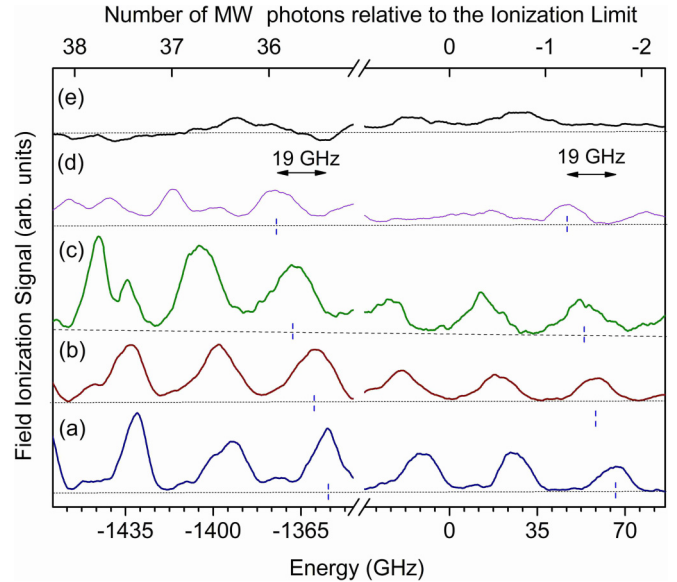

FIG. 5. (Color online) Field-ionization signal as a function of laser frequency tuning after exposure to a microwave pulse of 90 V/cm amplitude for different static fields in the interaction region: (a) 8 mV/cm, (b) 17 mV/cm, (c) 25 mV/cm, (d) 40 mV/cm, and (e) 55 mV/cm. A break is shown on the horizontal axis for convenience. Horizontal dashed lines show the baselines of the corresponding spectra. Vertical blue lines intersect the horizontal baselines at points to which the ionization limit is depressed due to $W = 2\sqrt{E}$ for the corresponding static field E. The double headed arrow that is 19 GHz long is the difference in the depression of the limit by 40 and 8 mV/cm fields. It is apparent that peaks in the microwave structure also shift by W, irrespective of the laser frequency. Increasing the static field destroys the microwave structure, and the 55-mV/cm spectrum shows only noise, with no bound population detected.

To determine the lifetimes of the atoms in the microwave field we increased the delay time between the third laser pulse and turning off the microwave field and recorded the number of bound atoms as a function of the delay for several laser wavelengths. Typical spectral peaks, at +60 and −2309 GHz, exhibit two component decays, as shown in Fig. 6. In the former case the initial fast decay time is 68(10) ns, and in the latter it is 107(10) ns. In all cases the slow decay time is longer than 1 μs, so we fit the experimental data to a rapidly decaying exponential plus a constant. When the laser is tuned midway between the peaks similar decay curves, but with much smaller amplitudes, are observed. There is no obvious dependence of the initial rapid decay on the microwave amplitude if the modulation in the spectrum is visible. With the exception of the long decay tie shown in Fig. 6, the decay times fall between 60 and 80 ns for all laser tunings.

IV. ONE-DIMENSIONAL QUANTUM SIMULATIONS

To provide further insight, we have carried out one-dimensional quantum calculations. The initial calculations were done for a microwave frequency of 38 GHz. While these calculations gave results in accord with the experimental results, they were barely converged, which precluded our probing subtle features with confidence. To circumvent this
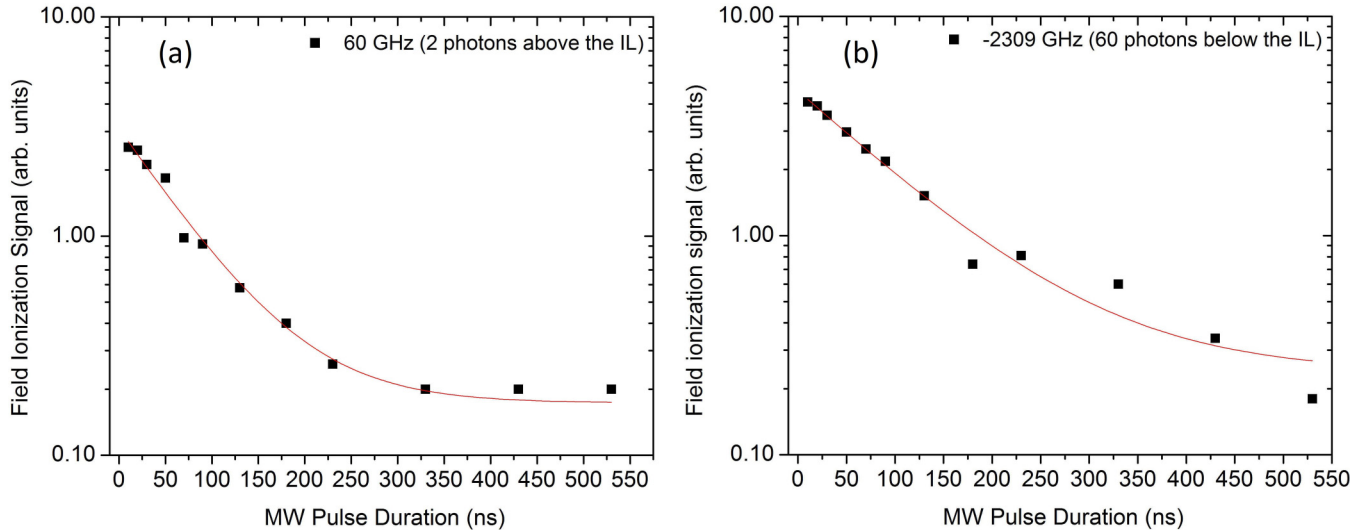
FIG. 6. (Color online) Field-ionization signal as a function of microwave pulse duration after the laser excitation. The microwave pulse amplitude is 90 V/cm, and the laser frequency is fixed and tuned to (a) two MW photons above the ionization limit and (b) 60 photons below it. Only the very high-lying states are collected with a 50-ns gate. The lifetimes exhibit an initial rapid decay followed by a very slowly decaying tail. The solid lines represent fits to the form $Ae^{-x/t} + c$. According to the fit, the lifetimes of decaying exponentials are 68(10) and 107(10) ns, respectively.

obstacle we scaled the problem. We have used n states a factor of 10 lower, $n \approx 20$ instead of 200, a microwave frequency of 38 THz instead of 38 GHz, and a field of 9×10^5 instead of 90 V/cm. With this scaling we are able to obtain well-converged results. We numerically solve the time-dependent Schrödinger equation using a Green's-function method with wave packets launched in a continuous wave (cw) microwave field. The time-dependent Schrödinger equation to be solved is

$$i \frac{\partial \psi(x,t)}{\partial t} - (H - E)\psi(x,t) = S(x,t), \qquad (1)$$

where H is the Hamiltonian and E is the energy at which the wave packet is launched, and the wave function $\psi(x,t)$ is initially zero everywhere. We use a Numerov scheme for our nonlinear spatial mesh to evolve Eq. (1) in time; as described in detail in Ref. [23]. The duration of the source term $S(x,t)$ is three microwave periods (giving ~ 8 THz at FWHM), and it has a Gaussian envelope in time. The wave packets are launched with energies ranging from -140 to 60 THz relative to the ionization threshold. We use a soft-core potential given by $V(x) = -1/\sqrt{x^2 + a^2}$ with $a = 1$ a.u. Since $V \to -1/|x|$ at large $|x|$, the potential has an infinite number of bound states. However, since the wave function exists for $x < 0$, there are twice as many states as in the H atom. The depth of the potential a has no direct consequence for the physical process of interest, the trapping of population in weakly bound states that have a spatial extent much larger than a.

The calculations lead to bound-state fractions similar to those seen in the experiment. In Fig. 7 we show the calculated spectra of bound atoms found after excitation in a 38-THz field of 9×10^5 V/cm. One might expect the spectra to correspond to those shown in Fig. 4(b). Specifically, we show the spectra for all remaining bound atoms (dotted blue curve) and those within one 38-THz photon of the ionization limit (solid red

curve). As shown by Fig. 7, the spectra are similar to the experimental spectra; peaks are found at the ionization limit modulo the microwave frequency. Figure 7 also provides information about the lifetime in the microwave field. When the atoms are exposed to longer 38-THz pulses the number
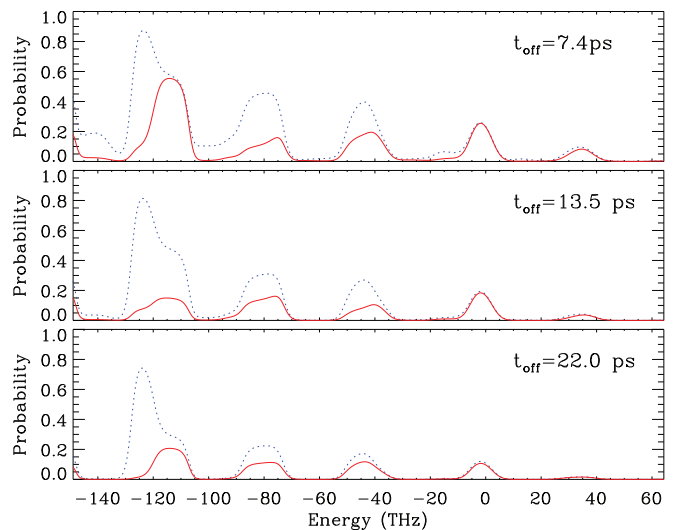

FIG. 7. (Color online) Calculated spectra for a 9×10^5-V/cm 38-THz field from scaled one-dimensional quantum simulations at three different turnoff times for the microwave field. We smoothly turn off the microwaves to mimic the experimental conditions and wait until the field strength drops below 10^{-8} V/cm before we compute the surviving norm. The dotted blue curves show the spectra obtained when all bound states are detected, and the solid red curves show the spectra obtained when only bound atoms within 38 THz of the limit are detected. These spectra should be compared to Fig. 4(b). The only difference should be the units of the horizontal scale, THz instead of GHz.
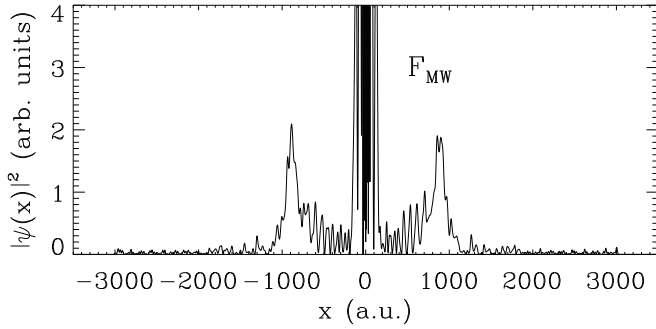
FIG. 8. The squared wave function 256 microwave cycles after the excitation pulse. There is substantial amplitude at small x and again at $x \sim \pm 900$ a.u. The peaks at ± 900 a.u. are persistent, whereas the small x part of the wave function decreases for sufficiently long microwave exposure. The peaks at $x = \pm 900$ a.u. are located at the classical turning points of $n = 21$.

of bound atoms decreases. An important point is that as the microwave pulse is lengthened the total number of bound atoms decreases more rapidly than the number of atoms within one microwave photon of the limit. When excitation occurs at the limit the high-lying states have a lifetime of approximately 18 ps. In view of the three-order-of-magnitude time scaling, this lifetime is consistent with the experimental lifetimes shown in Fig. 6. In long microwave pulses the bulk of the surviving atoms are in states whose energies are within one microwave photon of the limit, as observed experimentally. There are two differences between the calculated spectra of Fig. 7 and the experimental spectrum of Fig. 4(b). First, the peaks in the experimental spectrum extend much further above the ionization limit. Second, scaling the microwave frequency moves the resonance with the Kepler frequency relatively closer to the limit. For example, the $n = 9$ state lies at the energy -143 THz and the $n = 8$ to 9 frequency is 34 THz, nearly resonant with the 38-GHz field. As a result, the calculated spectra can be expected to exhibit irregularities similar to those in the spectrum of Fig. 4(b) at the energy of -1100 GHz.

The similarity of the calculated spectra to those observed experimentally gives us confidence that this simple model captures the essential physics of this system. Thus, we can use the wave function to help understand the unexpected stability of these states. Figure 8 shows the spatial probability distribution for the wave function within 3000 a_0 (here a_0 is the Bohr radius, .5 Å) of the nucleus 256 microwave cycles, 6.7 ps, after the excitation pulse. There is a large probability for the electron to be at $|x| \sim 900$ a_0, which corresponds to a few zero-field states of $n \sim 21$. A state with an outer turning point of ~ 900 a_0 is bound by 3.6 THz, a binding energy small compared to 38 THz. The $n = 21$ Kepler period is 2.8 ps, a factor of three shorter than the exposure time to the microwaves. As in the experiment, the electron remains bound even though it returns to the core during the microwave pulse. There is also substantial population at small x, a feature that is observed in the experiment only at small microwave fields and only for a range of initial binding energies where orbital frequency is larger than the microwave frequency. This population corresponds to $n \simeq 5$, where the

Kepler frequency is comparable to the microwave frequency. The population at small $|x|$ decays more rapidly than that at large $|x|$ and may be an intermediate state in ionization.

We have also performed one- and three-dimensional classical trajectory Monte Carlo simulations to further investigate the origin of this effect. However, in none of our classical simulations have we observed any surviving atoms, suggesting that the survival is entirely quantum mechanical in origin. Moreover, ~51% of all trajectories are within 38 GHz *above* the threshold. The classical piling up of the atoms within a single photon *above* threshold could mean piling up within a single photon *below* the threshold quantum mechanically. Unlike in classical mechanics, in quantum mechanics the electron has to absorb energy in discrete units (photons) and has to pass near the nucleus to absorb a photon. If the electron is in a state with a classical orbital period comparable to or larger than the microwave pulse duration, then quantum mechanically it will not have a chance to absorb the final necessary photon to escape. This, however, classically poses no problem for the escape of the electron, because when the electron acquires enough energy to put it within a photon of the threshold it only needs a fraction of a photon's energy to go above the threshold, which it can absorb continuously without need for passing close to the nucleus. Indeed, our quantum simulations have revealed this to be the mechanism for the survival of the atoms in the microwave field.

V. CONCLUSION

The spectra and calculations provide insight into why atoms survive the strong microwave field. Excitation is always to the ionization limit, modulo the microwave frequency, that is, to weakly bound Floquet states. Thus, an attractive alternative approach to this problem is the multichannel Floquet approach of Giusti-Suzor and Zoller [24]. In their approach there are multiple channels, each consisting of a Rydberg series and a continuum. Successive channels are displaced in energy by one microwave photon and are coupled by an electric dipole coupling. The Floquet eigenstates are linear superpositions of the wave functions of different channels and have both bound and continuum parts. In particular, the eigenstates contain bound states very close to the limit, deeply bound states multiples of the microwave frequency below the limit, and continua multiples of the microwave frequency above the limit. Due its having a continuum component, an initially bound eigenstate autoionizes into the continuum, just as in the quantum defect theory description of autoionizing states [25].

Atoms in high-lying states are not affected by the intense field if the electron does not return to the core during a laser pulse [1,4,5,19]. However, in the present case the electron clearly returns to the core during the microwave pulse since the Kepler orbital period T_K is short compared to the microwave pulse length. At 40 GHz below the limit $T_K = 3$ ns, and at the depressed limit imposed by an 8-mV/cm field it is 13 ns. Both times are far shorter than the observed 70- and 110-ns decay times. Due to the presence of an electric field, there is also an oscillation in ℓ, but its period is ~100 ns, long compared to the microwave pulse length, so it has minimal effect. However, the oscillation in ℓ or incoherent diffusion of

population to higher ℓ states may be the source of the long tails seen in the decay curves. Taken as a whole, the data suggest that atoms survive the microwave field because the Rydberg electron spends most of its time far from the core, where the strong microwave field only imposes a ponderomotive quiver on the electron's motion. A 38-GHz field of 90 V/cm leads to a quiver amplitude of 400 a_0, small compared to the 120 000-a_0 orbital size of an atom bound by 38 GHz. When the electron does come to the core it has an approximately equal chance of gaining or losing energy, so it is reasonable to expect atoms to survive several field cycles, as observed. Essentially the same result was observed in calculations to elucidate the source of superponderomotive electrons [15]; they are observed at the intensities which bring states just below the limit into multiphoton resonance with the ground state. In the usual case of ionization by a pulse of microwaves or laser light, the Stark shift due to the changing intensity during the pulse leads to resonant excitation of the high-lying states, as shown by the calculations of Muller [15]. Here we have explicitly shown the importance of resonant excitation by using laser excitation in the presence of a cw microwave field.

[1] R. R. Jones, D. W. Schumacher, and P. H. Bucksbaum, Phys. Rev. A **47**, R49 (1993).

[2] E. Wells, I. Ben-Itzhak, and R. R. Jones, Phys. Rev. Lett. **93**, 023001 (2004).

[3] P. Agostini, F. Fabre, G. Mainfray, G. Petite, and N. K. Rahman, Phys. Rev. Lett. **42**, 1127 (1979).

[4] R. R. Jones and P. H. Bucksbaum, Phys. Rev. Lett. **67**, 3215 (1991).

[5] H. Stapelfeldt, D. G. Papaioannou, L. D. Noordam, and T. F. Gallagher, Phys. Rev. Lett. **67**, 3223 (1991).

[6] C. I. Blaga, F. Catoire, P. Colosimo, G. G. Paulus, H. G. Muller, P. Agostini, and L. F. DiMauro, Nat. Phys. **5**, 335 (2008).

[7] W. Quan, Z. Lin, M. Wu, H. Kang, H. Liu, X. Liu, J. Chen, J. Liu, X. T. He, S. G. Chen *et al.*, Phys. Rev. Lett. **103**, 093001 (2009).

[8] L. Guo, S. S. Han, X. Liu, Y. Cheng, Z. Z. Xu, J. Fan, J. Chen, S. G. Chen, W. Becker, C. I. Blaga *et al.*, Phys. Rev. Lett. **110**, 013001 (2013).

[9] A. McPherson, G. Gibson, H. Jara, U. Johann, T. S. Luk, I. A. McIntyre, K. Boyer, and C. K. Rhodes, J. Opt. Soc. Am. B **4**, 595 (1987).

[10] D. N. Fittinghoff, P. R. Bolton, B. Chang, and K. C. Kulander, Phys. Rev. Lett. **69**, 2642 (1992).

[11] T. Nubbemeyer, K. Gorling, A. Saenz, U. Eichmann, and W. Sandner, Phys. Rev. Lett. **101**, 233001 (2008).

[12] U. Eichmann, A. Saenz, S. Eilzer, T. Nubbemeyer, and W. Sandner, Phys. Rev. Lett. **110**, 203002 (2013).

[13] W. C. Henneberger, Phys. Rev. Lett. **21**, 838 (1968).

[14] M. Pont, N. R. Walet, M. Gavrila, and C. W. McCurdy, Phys. Rev. Lett. **61**, 939 (1988).

[15] H. G. Muller, Phys. Rev. Lett. **83**, 3158 (1999).

[16] T. F. Gallagher, Phys. Rev. Lett. **61**, 2304 (1988).

[17] P. B. Corkum, N. H. Burnett, and F. Brunel, Phys. Rev. Lett. **62**, 1259 (1989).

[18] H. B. van Linden van den Heuvell and H. G. Muller, *Multiphoton Processes* (Cambridge University Press, Cambridge, 1988).

[19] A. Arakelyan and T. F. Gallagher, Phys. Rev. A **87**, 023410 (2013).

[20] J. H. Gurian, K. R. Overstreet, H. Maeda, and T. F. Gallagher, Phys. Rev. A **82**, 043415 (2010).

[21] E. S. Shuman, R. R. Jones, and T. F. Gallagher, Phys. Rev. Lett. **101**, 263001 (2008).

[22] K. R. Overstreet, R. R. Jones, and T. F. Gallagher, Phys. Rev. Lett. **106**, 033002 (2011).

[23] F. Robicheaux, J. Phys. B **45**, 135007 (2012).

[24] A. Giusti-Suzor and P. Zoller, Phys. Rev. A **36**, 5178 (1987).

[25] W. E. Cooke and C. L. Cromer, Phys. Rev. A **32**, 2725 (1985).